Central Washington University

ScholarWorks@CWU

All Faculty Scholarship for the College of the Sciences

College of the Sciences

4-14-2015

Twentieth century dust lows and the weakening of the westerly winds over the Tibetan Plateau

Bjorn Grigholm

P. A. Mayewski

S. Kang

Y. Zhang

U. Morgenstern

See next page for additional authors

Follow this and additional works at: https://digitalcommons.cwu.edu/cotsfac

Part of the Atmospheric Sciences Commons, Climate Commons, and the Geophysics and Seismology Commons

Authors
Bjorn Grigholm, P. A. Mayewski, S. Kang, Y. Zhang, U. Morgenstern, M. Schwikowski, Susan D. Kaspari, V. Aizen, E. Aizen, N. Takeuchi, K. A. Maasch, S. Birkel, M. Handley, and S. Sneed

AGU PUBLICATIONS

Geophysical Research Letters

RESEARCH LETTER
10.1002/2015GL063217

Key Points:
- Five hundred year calcium dust proxy was established from a Tibetan Plateau ice core
- Calcium and zonal wind correlations suggest a proxy for westerly wind strength
- Atmospheric dust and westerly strength are anomalously low in the twentieth century

Supporting Information:
- Texts S1–S10, Figures S1–S7, and Tables S1–S4
- Table S1
- Table S2
- Table S3
- Table S4
- Table S5
- Table S6

Correspondence to:
B. Grigholm,
bjorn.grigholm@maine.edu

Citation:
Grigholm, B., et al. (2015), Twentieth century dust lows and the weakening of the westerly winds over the Tibetan Plateau, *Geophys. Res. Lett.*, *42*, 2434–2441, doi:10.1002/2015GL063217.

Received 28 JAN 2015
Accepted 17 MAR 2015
Accepted article online 21 MAR 2015
Published online 14 APR 2015

Twentieth century dust lows and the weakening of the westerly winds over the Tibetan Plateau

B. Grigholm[1], P. A. Mayewski[1], S. Kang[2,3], Y. Zhang[2], U. Morgenstern[4], M. Schwikowski[5], S. Kaspari[6], V. Aizen[7], E. Aizen[7], N. Takeuchi[8], K. A. Maasch[1], S. Birkel[1], M. Handley[1], and S. Sneed[1]

[1]Climate Change Institute and School of Earth and Climate Sciences, University of Maine, Orono, Maine, USA, [2]State Key Laboratory of Cryospheric Sciences, Cold and Arid Regions Environmental and Engineering Research Institute, Chinese Academy of Sciences, Lanzhou, China, [3]CAS Center for Excellence in Tibetan Plateau Earth Sciences, Chinese Academy of Sciences, Beijing, China, [4]National Isotope Centre, Institute of Geological and Nuclear Sciences, Lower Hutt, New Zealand, [5]Paul Scherrer Institute, Villigen, Switzerland, [6]Department of Geological Sciences, Central Washington University, Ellensburg, Washington, USA, [7]Department of Geography, University of Idaho, Moscow, Idaho, USA, [8]Department of Earth Sciences, Graduate School of Science, Chiba University, Chiba, Japan

Abstract Understanding past atmospheric dust variability is necessary to put modern atmospheric dust into historical context and assess the impacts of dust on the climate. In Asia, meteorological data of atmospheric dust is temporally limited, beginning only in the 1950s. High-resolution ice cores provide the ideal archive for reconstructing preinstrumental atmospheric dust concentrations. Using a ~500 year (1477–1982 A.D.) annually resolved calcium (Ca) dust proxy from a Tibetan Plateau (TP) ice core, we demonstrate the lowest atmospheric dust concentrations in the past ~500 years during the latter twentieth century. Declines in late nineteenth to twentieth century Ca concentrations significantly correspond with regional zonal wind trends from two reanalysis models, suggesting that the Ca record provides a proxy for the westerlies. Twentieth century warming and attendant atmospheric pressure reductions over northern Asia have potentially reduced temperature/pressure gradients resulting in lower zonal wind velocities and associated dust entrainment/transport in the past ~500 years over the TP.

1. Introduction

Dust aerosols play an integral role in the climate system influencing the Earth's radiative balance directly (scattering and absorbing incoming/outgoing radiation, as well as modifying surface albedos) and indirectly (acting as cloud condensation nuclei and nutrients for marine ecosystems that impact global carbon cycles) [*Tegen et al.*, 1996; *Pruppacher and Klett*, 1978; *Mahowald et al.*, 2005]. Central Asia contains some of the Northern Hemisphere's largest sources of dust and is estimated to emit 10–30% of global emissions [*Tanaka and Chiba*, 2006; *Miller et al.*, 2004; *Werner et al.*, 2002] (see supporting information Text S1). The Central Asian Mountain System, which include the Pamirs, Hindu Kush, Tien Shan, Altai, the Himalayas, and the Tibetan Plateau (TP), provide excellent locations for reconstructing past atmospheric dust as it contains high-elevation glaciers that hold well-preserved ice core records [e.g., *Aizen et al.*, 2004; *Kang et al.*, 2002; *Kaspari et al.*, 2009; *Mayewski et al.*, 1984; *Takeuchi et al.*, 2009; *Thompson et al.*, 2006]. Herein we present a high-resolution, annually dated proxy record of atmospheric dust from a Mount Geladaindong (GL) ice core and investigate the variability and climatic controls of atmospheric dust on the TP over the last ~500 years.

2. Materials and Methods

In 2005 a 147 m ice was retrieved from Guoqu Glacier, located on the northern slope of Mount Geladaindong (GL) (33.58°N, 91.17°E, 5720 m above sea level). A total of 3585 coregistered samples were collected for major soluble ions (Na^+, K^+, Mg^{2+}, Ca^{2+}, Cl^-, NO_3^-, and SO_4^{2-}), major and trace elements (Ca, Al, S, Mg, Fe, K, Na, and Bi,) and stable isotopes ($\delta^{18}O$) (see supporting information Text S2). In addition, samples were collected for tritium and ^{210}Pb analysis [*Kang et al.*, 2015] (see supporting information Text S2).

The GL ice core was annually dated to 1477 at a depth of 109.93 m. Individual years were selected by identifying the seasonality of autumn-winter-spring peaks in major ion/element dust species (e.g., Ca, Al, Fe, and SO_4^{2-}) and the seasonality of $\delta^{18}O$-depleted summer monsoon precipitation (see supporting information Text S3). GL depth-age estimates are supported by ^{210}Pb, tritium, volcanic markers, and an ice flow model (see supporting

 ©2015. American Geophysical Union. All Rights Reserved.

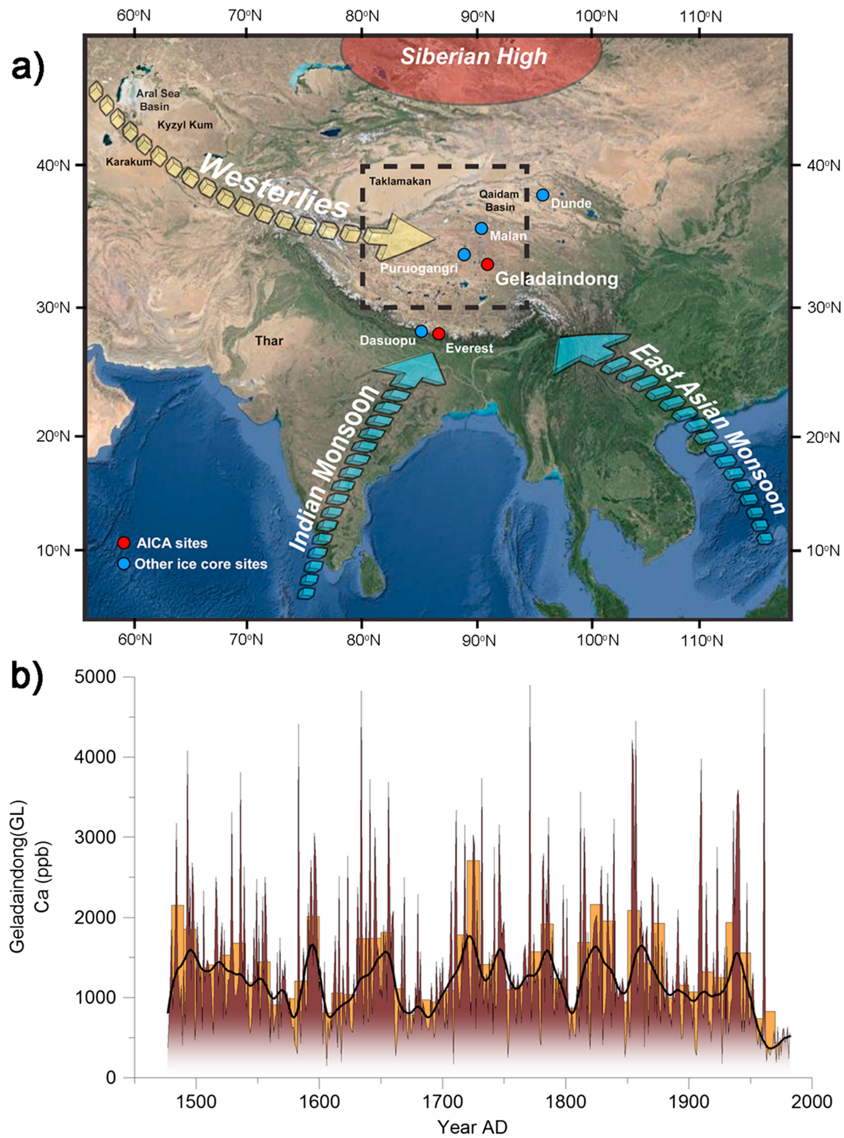

Figure 1. Research location and GL Ca dust proxy time series. (a) Map of study area and generalized atmospheric circulation: the westerlies, the Siberian High (SH), and Indian and East Asian components of Asian Summer Monsoon (ASM). TP_{grid} (30°N–40°N and 80°E–95°E) (dotted rectangle), Asian Ice Core Array (AICA) sites (red circles), and other ice cores (blue circles). (b) GL Ca concentrations 1477–1982. Annual (brown), 10 year means (yellow) and robust spline (tension 0.01) (black).

information). Dating uncertainties are estimated at ±0 years at 1963 based on the tritium peak and Agung eruption horizon, ±5 years at 1872 and ±20 years at 1477. Although the ice core was recovered in 2005, mass loss of snow and ice, due to ablation, at GL resulted in the removal of the most recent 23 years of the record yielding 1982 as the top year. Thus, the GL depth-age scale presented in this paper varies from previously published GL research interpreting a shallower 74 m ice core record from the same expedition in 2005 [e.g., *Zhang et al.*, 2007; *Grigholm et al.*, 2009; *Kang et al.*, 2010] (see supporting information Text S4).

3. Results and Discussion

The transport of atmospheric aerosols to GL is primarily dominated by westerly and the Siberian High (SH) circulation patterns as well as marine air masses associated with the Asian Summer Monsoon (ASM) [*Bryson*, 1986; *Aizen et al.*, 1996] (Figure 1a). The semiarid steppe and desert regions that cover the central and western portions of the TP [*Wang*, 1988] result in TP glaciochemistry that is dominated throughout the year by crustal dust, despite summer monsoon marine air mass incursions [e.g., *Cong et al.*, 2007; *Zhang et al.*, 2001;

©2015. American Geophysical Union. All Rights Reserved.

Li et al., 2007]. Empirical orthogonal function (EOF) analysis of GL major soluble ions (Na^+, K^+, Mg^{2+}, Ca^{2+}, Cl^-, NO_3^-, and SO_4^{2-}) clearly reflects the common variance/seasonality of crustal species as EOF 1 represents ~80% of the total specie variation. In addition, there are no eigenvectors loading with common marine tracers (i.e., Na^+ and Cl^-) and GL glaciochemical concentrations are an order of magnitude greater than Himalayan ice cores (e.g., Everest), which are closer to marine sources [*Kaspari et al.*, 2007] (see supporting information Text S5).

For this study, calcium (Ca and Ca^{2+}) concentrations were selected as the primary proxy for local atmospheric dust as it represents ~50% of total specie burdens (see Table S3). Calcium is commonly utilized as a dust proxy for ice core studies in the region [e.g., *Wake and Mayewski*, 1993; *Kreutz and Sholkovitz*, 2000; *Kang et al.*, 2002; *Kaspari et al.*, 2007]. Previous research on mass-particle size distributions from nearby Lhasa and Gongga indicate that Ca is strongly controlled by local TP sources, while other dust-derived elements (e.g., Al and Fe) are representative of distally transported dust [*Zhang et al.*, 2001]. The high concentrations of Ca are likely derived from the abundant calcareous soils that cover the TP and surround the GL site (see supplemental information Text S5).

The GL Ca time series from 1477 to 1982 are shown in Figure 1b. Annual concentrations are reported rather than flux (flux = concentration × accumulation rate) as dry versus wet deposition rates are not well constrained on the TP and there is no significant correlation between Ca concentrations and accumulation rates to justify a flux correction (see supporting information Text S6). Generally, the highest Ca concentrations in the GL records occur during the 1700s and 1800s (centennial means > 1500 ppb), while the lowest Ca concentrations occur during the 1900s, (centennial mean ~1150 ppb). Between 1480 and 1950, Ca concentrations are characterized by high decadal-to-multidecadal variability. This temporal pattern is abruptly altered ~1950 when Ca concentrations and variability decline significantly and remain low to the top of the record. The abrupt shift in atmospheric dust occurs ~1952–1956. The 1950–1980 mean concentration is ~670 ppb. This 30 year period has the lowest Ca concentrations in the entire record and is highlighted by the lowest decadal Ca concentrations of ~440 ppb between 1970 and 1980.

To assess the extent of the GL dust proxy record, comparisons were made to contemporary ice core dust proxy records on the TP (Dunde [*Takeuchi et al.*, 2009; *Yang et al.*, 2006], Malan [*Wang et al.*, 2006], and Puruogangri [*Thompson et al.*, 2006]), and in the Himalayas (i.e., Everest [*Kaspari et al.*, 2007] and Dasuopu [*Thompson et al.*, 2000]) (Figure 2a). TP dust proxies display distinct similarities to GL, including the lowest concentrations occurring between 1950 and 1980 (the only exception being two low dust periods (late 1500s and late 1600s) at Malan). GL, Dunde, and Malan reveal similar declining trends between 1850 and 1980, while dust declines occur ~50 years later in the Puruogangri record at ~1900. Puruogangri, Malan, and Dunde all extend beyond 1982 and show a continued decline in dust until ~2000. Linear regression generally reveals significant declining trends from the mid-1800s: GL (1850–1980, $r^2 = 0.43$, $p = 0.015$), Malan (1850–2000, $r^2 = 0.52$, $p = 0.002$), Dunde (1850–2000, $r^2 = 0.71$, $p > 0.001$), and Puruogangri (1900–2000, $r^2 = 0.56$, $p = 0.01$). In addition, correlations between GL with Malan and Dunde reveal strong associations, suggesting either similar dust sources and/or similar climatic controls (e.g., wind velocities) (see supporting information Text S7).

The prominent decline observed in TP dust proxy records post-1950 coincides with declines in dust storm (DS) observations across northern China [*Qian et al.*, 2002] and the TP (see supporting information Text S8). *Wang* [2005] reported the similarity of trends between northern China DS and the Malan core. In contrast, Himalayan ice cores, Everest, and Dasuopu, generally display increasing dust concentrations in the twentieth century. This increasing trend most likely represents non-TP dust sources (e.g., Thar Desert and/or the Arabian Peninsula), varying seasonal dust input, and/or anthropogenic activity (see supporting information Text S7). Twentieth century declines in DS in China have been attributed to varying climatic and/or anthropogenic mechanisms (e.g., wind strength, temperature gradients and cyclonic activity, precipitation and vegetation cover, and desertification and land management), although natural factors are primarily suggested [*Goudie*, 2009].

To help determine the physical mechanisms responsible for shifts in atmospheric dust at GL, we utilized reanalysis models National Centers for Environmental Prediction (NCEP) 1 (1948–1982) and Twentieth Century Reanalysis V2 (20CRV2) (1871–1982) [*Kalnay et al.*, 1996; *Compo et al.*, 2011] to compare climate variables (i.e., zonal wind, geopotential height (gph), precipitation, and temperature) to GL Ca concentrations (see supporting information Text S9). The 2.5° × 2.5° resolution of NCEP 1 and 20CRV2 gridded data cannot resolve all of the complex topography that may influence small-scale climate on the TP. However, researchers note much of the synoptic-scale climate variability in the Himalayan/TP region is captured using NCEP 1 [*Xie et al.*, 2007]. Therefore, we focus on regional-scale spatial and temporal climate relationships between

©2015. American Geophysical Union. All Rights Reserved.

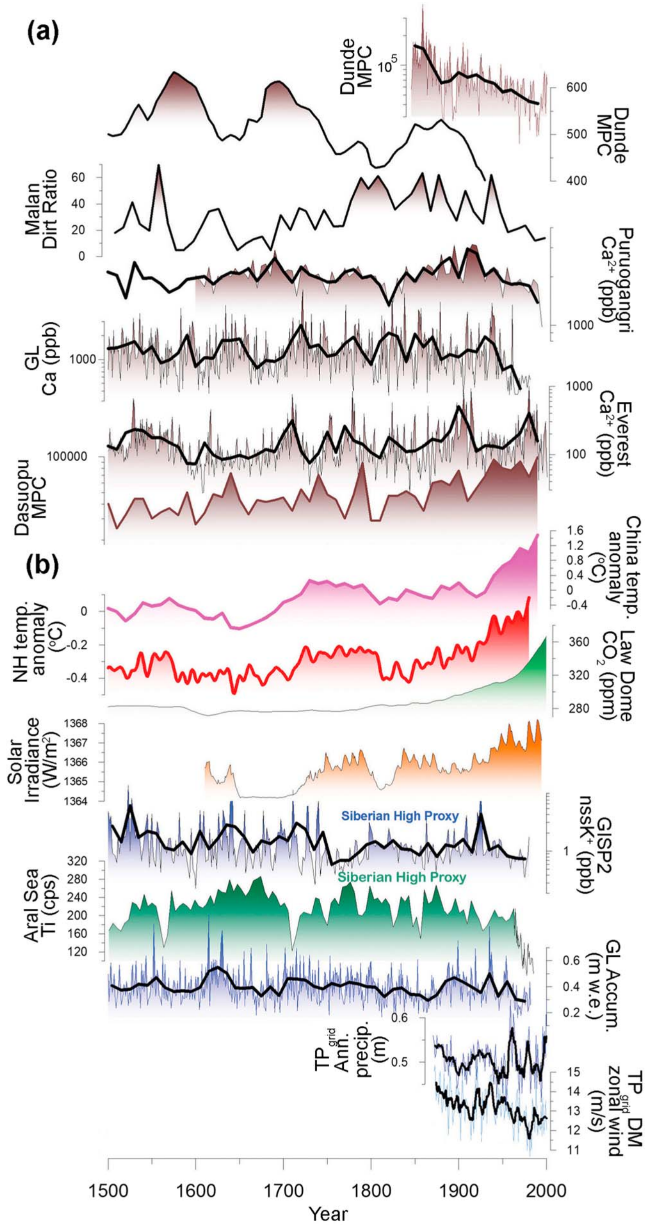

Figure 2. Climate proxies (1500–2000) and 20CRV2 data (1871–2000). (top to bottom) China temperature Anomaly, NH temperature Anomaly, Law Dome CO_2, solar irradiance, GISP2 $nssK^+$, Aral Sea Ti, GL accumulation, 20CRV2 TP_{grid} Dust Months (DM) precipitation, 20CRV2 TP_{grid} DM zonal $wind_{400\ mbar}$, Dunde $MPC^{1850–2000}$ (0.52–16 μm), Dunde $MPC^{1500–1930}$; Malan Dirt Ratio, Puruogangri Ca^{2+} (brown), GL Ca (brown), Everest Ca^{2+}, and Dasuopu MPC.

GL Ca records and climate variables. The reanalysis data are available at the NOAA Earth System Research Laboratory website (http://www.esrl.noaa.gov/psd/data/gridded/). Annual GL Ca concentrations were correlated to climate variables during the months of primary DS activity (November–May), referred hereon as dust months (DM) [*Han et al.*, 2004]. In addition, correlations were conducted on nondust months (NDM) (June–October), as well as the full calendar year (January–December), to test relationships when atmospheric aerosols are at baseline concentrations and to capture total annual variations, respectively. 20CRV2 correlations were calculated for annual, 5 year, and 10 year means. Multiyear averages were utilized to account for interannual variability, to better assess long-term trends, as well as to account for possible dating errors. Due to the lognormal distribution of the GL Ca time series, the log transformation is used in the correlation analysis.

NCEP1 (1949–1982) spatial DM correlation maps reveal that zonal winds have the strongest correlations to GL logCa. Significant positive correlations are found over the majority of the TP, with the strongest correlations ($r = 0.52$, $p = 0.002$) directly west of GL (Figure 3a). NOAA Hybrid Single-Particle Lagrangian Integrated Trajectory (HYSPLIT) model back trajectory frequency analysis reveal that during DM the majority of air masses originate from the west, clearly corresponding to the highest zonal wind correlation values on the TP (Figure 3b). The zonal wind: logCa relationship suggests that as wind velocities increase/decrease, transport of dust species west of GL is strengthened/weakened. Significant spatial correlations were not observed for the other climate parameters, with the exception of perhaps NDM temperature. NDM temperatures display positive significant correlation to the north and east but not to the west where dust primarily originates (see supporting information Text S9). It is important to note that the resolution of NCEP 1 grids may not capture the complex spatial distribution of precipitation patterns that may influence dust transport. Therefore, GL Ca was also compared to precipitation records from two local weather stations: Tuotuohe station to the northeast (34.23°N; 94.44°E; 1956–1982) and Amdo station to the southwest (31.15°N; 97.16°E; 1966–1982) (National Climate Center, China Meteorological Administration). No correlations were found for DM or NDM to suggest a precipitation control on GL Ca.

 ©2015. American Geophysical Union. All Rights Reserved.

Table 1. GL logCa TPgrid (30°–40°N: 80°–95°E) Reanalysis Correlations

Climate Variable	NCEP 1 1948–1982		20CRV2 1871–1982					
DM	Annual $n = 34$		Annual $n = 111$		5 year $n = 22$		10 year $n = 11$	
	r	p Value[a]	r	p Value	r	p Value	r	p Value
Zonal wind$_{400\ mbar}$	0.41	0.02	0.35	<0.001	0.62	0.002	0.78	0.005
Zonal wind$_{500\ mbar}$	0.43	<0.01	0.32	<0.001	0.46	0.03	0.6	0.05
Precipitation$_{surface}$	0.3		−0.31	<0.001	−0.22		0.21	
gph$_{500\ mbar}$	−0.09		0.024		−0.18		0.04	
Temperature$_{surface}$	−0.14		0.09		0.05		0.31	
Annual	Annual $n = 35$		Annual $n = 111$		5 year $n = 22$		10 year $n = 11$	
	r	p Value	r	p Value	r	p Value	r	p Value
Zonal wind$_{400\ mbar}$	0.23		0.24	0.01	0.51	0.02	0.73	0.01
Zonal wind$_{500\ mbar}$	0.33	0.05	0.15		0.23		0.36	
Precipitation$_{surface}$	0.23		−0.06		0.15		0.37	
gph$_{500\ mbar}$	−0.17		−0.1		−0.16		−0.38	
Temperature$_{surface}$	−0.04		0.06		0.15		0.38	
NDM	Annual $n = 35$		Annual $n = 111$		5 year $n = 22$		10 year $n = 11$	
	r	p Value	r	p Value	r	p Value	r	p Value
Zonal wind$_{400\ mbar}$	−0.08		−0.15		−0.25		−0.33	
Zonal wind$_{500\ mbar}$	0.08		0.09		−0.18		−0.12	
Precipitation$_{surface}$	−0.07		0.04		−0.08		0.1	
gph$_{500\ mbar}$	0.03		0.15		−0.26		−0.55	0.08
Temperature$_{surface}$	0.44	<0.01	0.01		−0.19		−0.45	

[a]p values are two tail, and only p values ≤ 0.1 are reported.

20CRV2 (1871–1982) extracted time series also suggest that DM zonal wind is the dominant control on TP atmospheric dust, exhibiting significant correlations for annual, 5 year, and 10 year mean logCa (Table 1). The increased correlation strength with longer time averages (i.e., $r_{annual} = 0.35$ ($p < 0.001$); $r_{5\ year} = 0.62$ ($p < 0.01$); and $r_{10\ year} = 0.78$ ($p < 0.01$)) suggests that the zonal wind proxy is a more robust interpretation on a decadal timescale, as it better accounts for interannual climatic controls of atmospheric dust, as well as potential dating errors. 20CRV2 zonal wind correlations are stronger at higher elevations, suggesting that enhanced/weakened

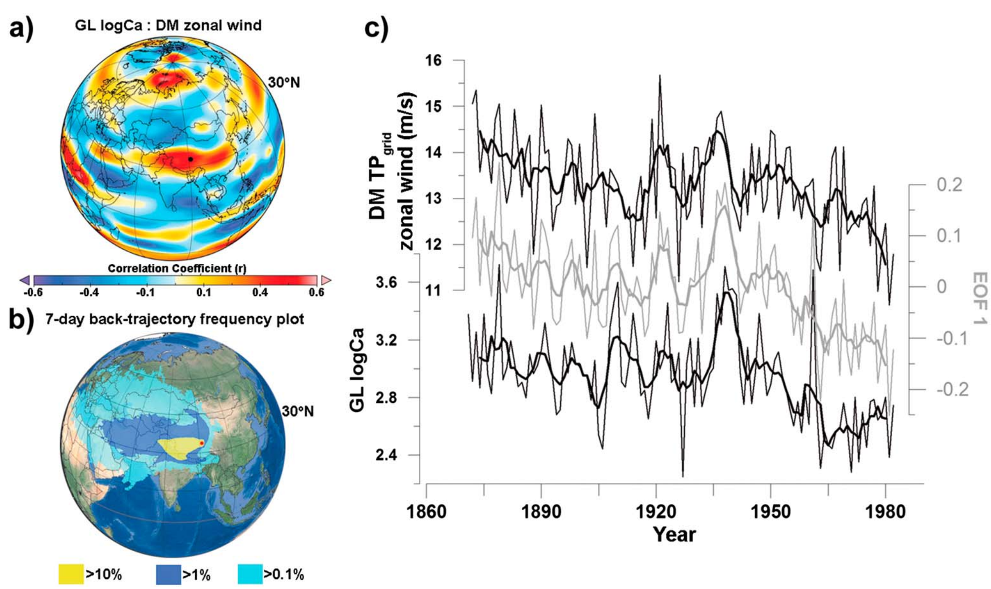

Figure 3. Atmospheric circulation and GL logCa comparisons. (a) Spatial correlations of GL logCa and NCEP 1 DM zonal wind$_{500\ mbar}$. GL site (black circle) (highest values ($n = 34$; $r = 0.52$; $p = 0.002$) due west of GL). (b) NOAA HYSPLIT 7 day back trajectory frequency plot for DM (1950–1980). GL (red circle). (c) 20CRV2 TP$_{grid}$ DM zonal wind$_{400\ mbar}$, GL logCa, and their common EOF 1, representing 68% of the variance in the two time series.

©2015. American Geophysical Union. All Rights Reserved.

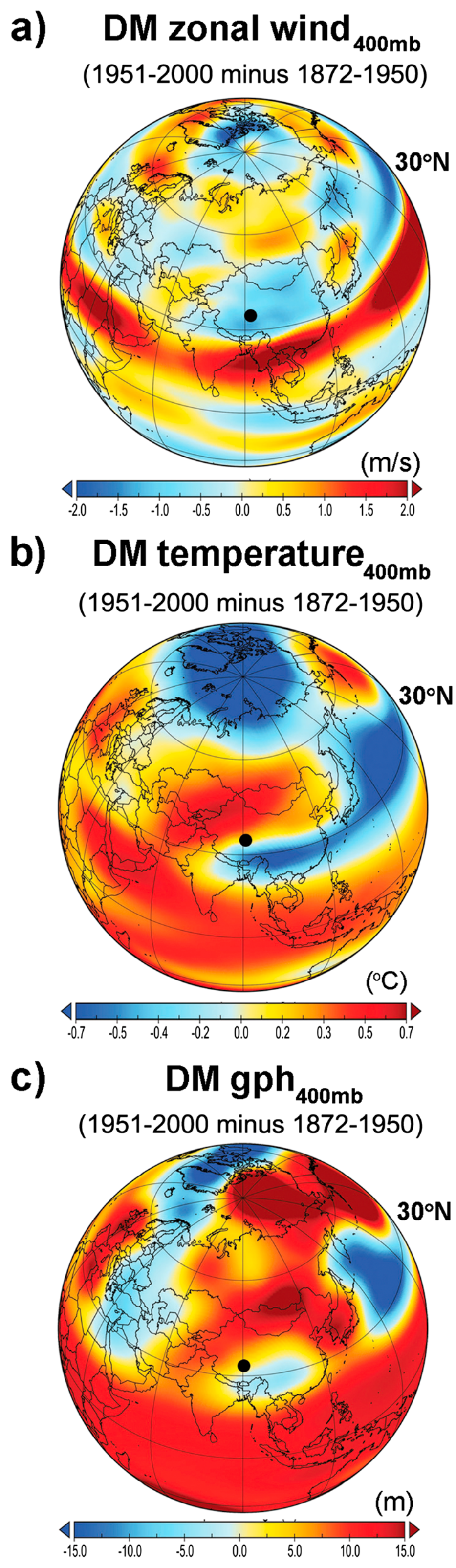

Figure 4. 20CRV2 $DM_{400\ mbar}$ difference maps (1951–2000 minus 1872–1950). (a) Zonal wind, (b) temperature, and (c) gph.

upper air transport may be more responsible for higher/lower Ca concentrations than aerosol entrainment at the dust source (see supporting information Text S9). To illustrate the temporal relationship between logCa and TP_{grid} zonal wind, EOF analysis was conducted and revealed a common variance of 68% (Figures 3c). In addition, to exclude biases from long-term trends in the data, correlation, and EOF analysis were conducted on detrended logCa and TP_{grid} zonal wind, which also revealed significant direct associations (i.e., $r_{annual} = 0.23$ ($p = 0.015$); $r_{5\ year} = 0.45$ ($p = 0.03$); and $r_{10\ year} = 0.57$ ($p = 0.06$)) and a common variance of 62%. Significant spatial correlations were not observed for the other climate parameters. We also utilized regional ice core (i.e., Everest, Guliya, Dunde, Puruogangri, Dasuopu, and GL) net accumulation proxies to assess the potential impact of past precipitation trends on atmospheric dust. These potential precipitation proxies revealed no relationship to the GL Ca dust proxy (see supplemental information Text S10).

The similarity in twentieth century TP dust proxies and zonal wind suggests that the westerlies are most likely the primary control on dust transport. To spatially illustrate the likely regional mechanisms responsible for the weakening of the westerlies, 20CRV2 400 mbar zonal wind, temperature, and gph difference maps are presented (Figure 4). The year 1950 was utilized as a demarcation for the difference maps as it is associated with a significant shift in atmospheric dust concentrations at GL. 20CRV2 difference maps illustrate how 1951–2000 DM warming over north central Asia, northwestern China, Mongolia, and Siberia (an area strongly influenced by the SH) has increased the regional gph relative to the 1872–1950 period (Figures 4b and 4c). Difference maps suggest that the SH has weakened, resulting in reduced meridional pressure gradients over the TP and lower zonal wind velocities, which reduce dust transport over the TP. In addition, difference maps reveal slight declines in gph over the eastern TP, which may also reduce zonal winds via atmospheric blocking.

To test the potential of a long-term GL Ca westerly proxy, we compared the GL Ca record to regional-global-scale forcing proxy data (i.e., China temperature anomaly [*Yang et al.*, 2002], Northern Hemisphere (NH) temperature anomaly [*Mann and Jones*, 2003], Law Dome CO_2 [*Etheridge et al.*, 1996], solar irradiance [*Lean et al.*, 1995], and the SH [*Meeker and Mayewski*, 2002; *Sorrel et al.*, 2007], that may explain pre-reanalysis trends in TP zonal winds and atmospheric dust (Figure 2b). GL Ca generally displays an inverse relationship to temperature anomaly proxies from China and the NH with higher Ca periods (i.e., 1500s to mid-1800s) corresponding to colder periods (primarily forced by solar irradiance) and lower Ca periods (i.e., mid-1800s to late 1900s) corresponding with warmer periods (primarily forced by anthropogenic CO_2 emissions). Comparisons with two SH proxy records derived from a

©2015. American Geophysical Union. All Rights Reserved.

Greenland Ice Sheet Project 2 non-sea-salt K^+ (GISP2 nssK^+) record [*Meeker and Mayewski*, 2002] and an Aral Sea Ti sediment core proxy [*Sorrel et al.*, 2007] also reflect an inverse relationship to temperature proxies. This suggests, as reanalysis models, that colder/warmer periods drive a stronger/weaker SH and are likely responsible for zonal wind strengths and dust transport on the TP. The relationships between the proxy records are most prominently highlighted during the middle-late twentieth century when anthropogenic CO_2 concentrations and temperature proxies are the highest and correspond to the weakest SH and zonal wind strengths, as well as the lowest TP dust concentrations in last ~500 years.

The anomalously low post-1950s GL Ca concentrations (~50% below 1480–1950 concentrations) correspond with the anthropogenic warming of the middle-late twentieth century. As warming continues, temperature/pressure gradients driving the westerlies will presumably decline [*Francis and Vavrus*, 2012], as will, most likely, the transport of dust. Therefore, future trends of atmospheric dust over the TP may be more dominantly controlled by other factors (e.g., precipitation, source area, and/or anthropogenic activity). For example, twentieth century warming combined with poor land management has increased land degradation and desertification, exposing more sediments to possible entrainment [*Wang et al.*, 2000; *Gong et al.*, 2004]. In addition, studies estimated that between the 1950s and 1990s China's desert regions increased by ~2–7% and would yield 10–40% more DS under 1950s atmospheric conditions (i.e., stronger wind strengths) [*Zhong*, 1999; *Zhu and Zhu*, 1999]. Importantly, the GL Ca dust proxy provides a longer historical perspective and insight into the preinstrumental era, strongly suggesting that if atmospheric circulation strengths returned to a pre-1950s state, even greater DS frequency would be expected.

4. Conclusion

This paper presents a high-resolution ~500 year Ca record (1477–1982) from GL that provides a proxy for atmospheric dust concentrations and westerly wind strength over the TP. Late nineteenth to twentieth century declines in Ca concentrations correspond with regional trends in reduced zonal wind strengths. Significant positive DM (November–May) correlations between logCa and NCEP 1 (1949–1982) and 20CRV2 (1872–1982) zonal wind velocities indicate that the GL record yields a proxy for the strength of the westerlies. Twentieth century declines in zonal wind velocities, and the subsequent declines in dust transport over the TP, are likely the result of increased DM temperatures lowering meridional pressure gradients (i.e., weakening the SH) over large portions of northern Asia. Additionally, the GL Ca record displays a decadal-centennial relationship with regional temperature proxies and SH proxies, reflecting the long-term control of regional atmospheric circulation strength over atmospheric dust concentrations on the TP.

Acknowledgments
This research was supported by the NSF ATM 0754644 as part of the AICA (Asian Ice Core Array) project, the NSF P2C2 1401899 and the NSF Adaptation to Abrupt Climate Change IGERT program DGE-1144423. The GL ice core data for Figures 1–3 are available as data set files in the supporting information. Support for the Twentieth Century Reanalysis Project data set is provided by the U.S. Department of Energy, the Office of Science Innovative and Novel Computational Impact on Theory and Experiment (DOE INCITE) program, the Office of Biological and Environmental Research (BER), and the National Oceanic and Atmospheric Administration Climate Program Office. The authors gratefully acknowledge the NOAA Air Resources Laboratory (ARL) for the provision of the HYSPLIT transport and dispersion model and/or READY website (http://www.ready.noaa.gov) used in this publication.

The Editor thanks Ian Goodwin and an anonymous reviewer for their assistance in evaluating this paper.

References

Aizen, V., E. Aizen, J. Melack, and T. Martma (1996), Isotopic measurements of precipitation on central Asian glaciers (southeastern Tibet, northern Himalayas, central Tien Shan), *J. Geophys. Res.*, *101*(D4), 9185–9196, doi:10.1029/96JD00061.

Aizen, V., E. M. Aizen, J. M. Melack, K. J. Kreutz, and L. D. Cecil (2004), Association between atmospheric circulation patterns and firn-ice core records from the Inilchek glacierized area, central Tien Shan, Asia, *J. Geophys. Res.*, *109*, D08304, doi:10.1029/2003JD003894.

Bryson, R. A. (1986), Airstream climatology of Asia, proceedings of the International Symposium on the Qinghai-Xizang Plateau and mountain meteorology, March 20–24, 1984, Beijing, China: Boston, Mass, *Am. Meteorol. Soc.*, 604–617.

Compo, G. P., et al. (2011), The Twentieth Century Reanalysis Project, *Q J. R. Meteorol. Soc.*, *137*(654), 1–28, doi:10.1002/qj.776.

Cong, Z. Y., S. C. Kang, X. D. Liu, and G. F. Wang (2007), Elemental composition of aerosol in the Nam Co region, Tibetan Plateau, during summer monsoon season, *Atmos. Environ.*, *41*, 1180–1187, doi:10.1016/j.atmosenv.2006.09.046.

Etheridge, D. M., L. P. Steele, R. L. Langenfelds, R. J. Francey, J.-M. Barnola, and V. I. Morgan (1996), Natural and anthropogenic changes in atmospheric CO_2 over the last 1000 years from air in Antarctic ice and firn, *J. Geophys. Res.*, *101*, 4115–4128, doi:10.1029/95JD03410.

Francis, J. A., and S. J. Vavrus (2012), Evidence linking Arctic amplification to extreme weather in mid-latitudes, *Geophys. Res. Lett.*, *39*, L06801, doi:10.1029/2012GL051000.

Gong, S. L., X. Y. Zhang, T. L. Zhao, and L. A. Barrie (2004), Sensitivity of Asian dust storm to natural and anthropogenic factors, *Geophys. Res. Lett.*, *31*, L07210, doi:10.1029/2004GL019502.

Goudie, A. S. (2009), Dust storms: Recent developments, *J. Environ. Manage.*, *90*(1), 89–94, doi:10.1016/j.jenvman.2008.07.007.

Grigholm, B., P. A. Mayewski, S. Kang, Y. Zhang, S. Kaspari, S. B. Sneed, and Q. Zhang (2009), Atmospheric soluble dust records from a Tibetan ice core: Possible climate proxies and teleconnection with the Pacific Decadal Oscillation, *J. Geophys. Res.*, *114*, D20118, doi:10.1029/2008JD011242.

Han, Y., X. Xi, and L. Song (2004), Spatio-temporal sand-dust distribution in Qinghai-Tibet Plateau and its climatic significance, *J. Desert Res.*, *24*, 588–592.

Kalnay, E., et al. (1996), The NCEP/NCAR 40-year reanalysis project, *Bull. Am. Meteorol. Soc.*, *77*, 437–470, doi:10.1175/1520-0477(1996)077<0437:TNYRP>2.0.CO;2.

Kang, S., P. A. Mayewski, D. Qin, Y. Yan, S. Hou, D. Zhang, J. Ren, and K. Kruetz (2002), Glaciochemical records from a Mt. Everest ice core: Relationship to atmospheric circulation over Asia, *Atmos. Environ.*, *36*(21), 3351–3361.

Kang, S., Y. Zhang, Y. Zhang, B. Grigholm, S. Kaspari, D. Qin, J. Ren, and P. Mayewski (2010), Variability of atmospheric dust loading over the central Tibetan Plateau based on ice core glaciochemistry, *Atmos. Environ.*, *44*(25), 2980–2989, doi:10.1016/j.atmosenv.2010.05.014.

 ©2015. American Geophysical Union. All Rights Reserved.

Kang, S., et al. (2015), Decapitation of high-altitude glaciers on the Tibetan Plateau revealed by ice core tritium and mercury records, *Cryosphere Discuss.*, *9*, 417–440, doi:10.5194/tcd-9-417-2015.

Kaspari, S., et al. (2007), Reduction in northward incursions of the South Asian monsoon since ~ 1400 AD inferred from a Mt. Everest ice core, *Geophys. Res. Lett.*, *34*, L16701, doi:10.1029/2007GL030440.

Kaspari, S., P. A. Mayewski, M. Handley, S. Kang, S. Hou, S. Sneed, K. Maasch, and D. Qin (2009), A high-resolution record of atmospheric dust composition and variability since a.d.1650 from a Mount Everest ice core, *J. Clim.*, *22*(14), 3910–3925, doi:10.1175/2009JCLI2518.1.

Kreutz, K. J., and E. R. Sholkovitz (2000), Major element, rare earth element, and sulfur isotopic composition of a high-elevation firn core: Sources and transport of mineral dust in Central Asia, *Geochem., Geophys., Geosyst.*, *1*(11), 1048, doi:10.1029/2000GC000082.

Lean, J., J. Beer, and R. Bradley (1995), Reconstruction of Solar Irradiance Since 1610: Implications for Climate Change, *Geophys. Res. Lett.*, *22*(23), 3195–3198, doi:10.1029/95GL03093.

Li, C., S. Kang, Q. Zhang, and S. Kaspari (2007), Major ionic composition of precipitation in the Nam Co region, central Tibetan Plateau, *Atmos. Res.*, *85*, 351–360, doi:10.1016/j.atmosres.2007.02.006.

Mahowald, N. M., A. R. Baker, G. Bergametti, N. Brooks, R. A. Duce, T. D. Jickells, N. Kubilay, J. M. Prospero, and I. Tegen (2005), Atmospheric global dust cycle and iron inputs to the ocean, *Global Biogeochem. Cycles*, *19*, GB4025, doi:10.1029/2004GB002402.

Mann, M. E., and P. D. Jones (2003), Global surface temperatures over the past two millennia, *Geophys. Res. Lett.*, *30*(15), 1820, 10.1029/2003GL017814.

Mayewski, P. A., N. Ahmad, G. Smith, and M. Pourchet (1984), Interpretation of the chemical and physical time-series retrieved from Sentik Glacier, Ladakh Himalaya, India, *J. Glaciol.*, *30*, 66–76.

Meeker, L. D., and P. A. Mayewski (2002), A 1400-year high-resolution record of atmospheric circulation over the North Atlantic and Asia, *Holocene*, *12*(3), 257–266, doi:10.1191/0959683602hl542ft.

Miller, R. L., J. Perlwitz, and I. Tegen (2004), Modeling Arabian dust mobilization during the Asian summer monsoon: The effect of prescribed versus calculated SST, *Geophys. Res. Lett.*, *31*, L22214, doi:10.1029/2004GL020669.

Pruppacher, H. R., and J. K. Klett (1978), *Microphysics of Clouds and Precipitation*, Atmos. Oceanogr. Sci. Libr., vol. 18, Springer, Dordrecht, Heidelberg, London, New York.

Qian, W., L. Quan, and S. Shi (2002), Variations of the dust storm in China and its climatic control, *J. Clim.*, *15*(10), 1216–1229, doi:10.1175/1520-0442(2002)015<1216:VOTDSI>2.0.CO;2.

Sorrel, P., H. Oberhänsli, N. Boroffka, D. Nourgaliev, P. Dulski, and U. Röhl (2007), Control of wind strength and frequency in the Aral Sea basin during the late Holocene, *Quat. Res.*, *67*(3), 371–382, doi:10.1016/j.yqres.2006.12.003.

Takeuchi, N., T. Miyake, F. Nakazawa, H. Narita, K. Fujita, A. Sakai, M. Nakawo, Y. Fujii, K. Duan, and T. Yao (2009), A shallow ice core re-drilled on the Dunde Ice Cap, western China: Recent changes in the Asian high mountains, *Environ. Res. Lett.*, *4*(4), 045207, doi:10.1088/1748-9326/4/4/045207.

Tanaka, T. Y., and M. Chiba (2006), A numerical study of the contributions of dust source regions to the dust source regions to the global dust budget, *Global Planet. Change*, *52*(1–4), 88–104, doi:10.1016/j.gloplacha.2006.02.002.

Tegen, I., A. A. Lacis, and I. Fung (1996), The influence on climate forcing of mineral aerosols from disturbed soils, *Nature*, *380*, 419–422, doi:10.1038/380419a0.

Thompson, L. G., T. Yao, E. Mosley-Thompson, M. E. Davis, K. A. Henderson, and P. Lin (2000), A high-resolution millennial record of the South Asian Monsoon from Himalayan ice cores, *Science*, *289*(5486), 1916–1919, doi:10.1126/science.289.5486.1916.

Thompson, L. G., T. Yao, M. E. Davis, E. Mosley-Thompson, T. A. Mashiotta, P.-N. Lin, V. N. Mikhalenko, and V. S. Zagorodnov (2006), Holocene climate variability archived in the Puruogangri ice cap on the central Tibetan Plateau, *Ann. Glaciol.*, *43*(1), 61–69, doi:10.3189/172756406781812357.

Wake, C. P., and P. A. Mayewski (1993), The spatial variation of Asian dust and marine aerosol contributions to glaciochemical signals in central Asia, Proceedings of the International Symposium on Snow and Glacier Hydrology, Kathmandu, Nepal, 16–21 November, 1992, *IASH Publ.*, *218*, 385–402.

Wang, J. (1988), The steppes and deserts of the Xizang Plateau (Tibet), *Vegetatio*, *75*(3), 135–142.

Wang, N. (2005), Decrease trend of dust event frequency over the past 200 years recorded in the Malan ice core from the northern Tibetan Plateau, *Chin. Sci. Bull.*, *50*(24), 2866–2871.

Wang, S., H. Jin, S. Li, and L. Zhao (2000), Permafrost degradation on the Qinghai-Tibet Plateau and its environmental impacts, *Permafrost Periglacial Processes*, *11*, 43–53, doi:10.1002/(SICI)1099-1530(200001/03)11:1<43::AID-PPP332>3.0.CO;2-H.

Wang, N., T. Yao, L. G. Thompson, and M. E. Davis (2006), Strong negative correlation between dust event frequency and air temperature over the northern Tibetan Plateau reflected by the Malan ice-core record, *Ann. Glaciol.*, *43*(1), 29–33, doi:10.3189/172756406781812339.

Werner, M., I. Tegen, S. P. Harrison, K. E. Kohfeld, I. C. Colin, Y. Balkanski, H. Rodhe, and C. Roelandt (2002), Seasonal and interannual variability of the mineral dust cycle under present and glacial climate conditions, *J. Geophys. Res.*, *107*(D24), 4744, doi:10.1029/2002JD002365.

Xie, A., J. Ren, X. Qin, and S. Kang (2007), Reliability of NCEP/NCAR reanalysis data in the Himalayas/Tibetan Plateau, *J. Geogr. Sci.*, *17*(4), 421–430, doi:10.1007/s11442-007-0421-2.

Yang, B., A. Braeuning, K. R. Johnson, and S. Yafeng (2002), General characteristics of temperature variation in China during the last two millennia, *Geophys. Res. Lett.*, *29*(9), 1324, doi:10.1029/2001GL014485.

Yang, M., T. Yao, and H. Wang (2006), Microparticle content records of the Dunde ice core and dust storms in northwestern China, *J. Asian Earth Sci.*, *27*(2), 223–229, doi:10.1016/j.jseaes.2005.03.007.

Zhang, X. Y., R. Arimoto, J. J. Cao, Z. S. An, and D. Wang (2001), Atmospheric dust aerosol over the Tibetan Plateau, *J. Geophys. Res.*, *106*, 18, 471–18, 476, doi:10.1029/2000JD900672.

Zhang, Y., S. C. Kang, D. H. Qin, B. Grigholm, and P. A. Mayewski (2007), Changes in annual accumulation retrieved from Geladaindong ice core and its relationship to atmospheric circulation over the Tibetan Plateau, *Chin. Sci. Bull.*, *52*(23), 3261–3266.

Zhong, D. C. (1999), The dynamic changes and trends of modern desert in China [in Chinese], *Adv. Earth Sci.*, *14*, 230–234.

Zhu, J. F., and Z. D. Zhu (1999), *Combating Desertification in China* [in Chinese], Chinese Forest Press, Beijing.

 ©2015. American Geophysical Union. All Rights Reserved.